**Atmospheric
Chemistry
and Physics
Discussions**

Air pollution and associated human mortality: the role of air pollutant emissions, climate change and methane concentration increases during the industrial period

Y. Fang[1], V. Naik[2], L. W. Horowitz[2], and D. L. Mauzerall[1,3]

[1]Program in Science, Technology and Environmental Policy, Woodrow Wilson School of Public and International Affairs, Princeton University, Princeton, NJ, 08540, USA
[2]Geophysical Fluid Dynamics Laboratory, Princeton, NJ, 08540, USA
[3]Department of Civil and Environmental Engineering, Princeton University, Princeton, NJ, 08540, USA

Title Page

Abstract	Introduction
Conclusions	References
Tables	Figures

|◄ | ►|
◄ | ►

Back | Close

Full Screen / Esc

Printer-friendly Version

Interactive Discussion

Abstract

Increases in surface ozone (O_3) and fine particulate matter ($\leq 2.5\,\mu m$ aerodynamic diameter, $PM_{2.5}$) are associated with excess premature human mortalities. Here we estimate changes in surface O_3 and $PM_{2.5}$ since preindustrial (1860) times and the global present-day (2000) premature human mortalities associated with these changes. We go beyond previous work to analyze and differentiate the contribution of three factors: changes in emissions of short-lived air pollutants, climate change, and increased methane (CH_4) concentrations, to air pollution levels and the associated premature mortalities. We use a coupled chemistry-climate model in conjunction with global population distributions in 2000 to estimate exposure attributable to concentration changes since 1860 from each factor. Attributable mortalities are estimated using health impact functions of long-term relative risk estimates for O_3 and $PM_{2.5}$ from the epidemiology literature. We find global mean surface $PM_{2.5}$ and health-relevant O_3 (defined as the maximum 6-month mean of 1-h daily maximum O_3 in a year) have increased by $8 \pm 0.16\,\mu g\,m^{-3}$ and $30 \pm 0.16\,\mathrm{ppbv}$, respectively, over this industrial period as a result of combined changes in emissions of air pollutants (EMIS), climate (CLIM) and CH_4 concentrations (TCH4). EMIS, CLIM and TCH4 cause global average $PM_{2.5}$(O_3) to change by $+7.5 \pm 0.19\,\mu g\,m^{-3}$ ($+25 \pm 0.30\,\mathrm{ppbv}$), $+0.4 \pm 0.17\,\mu g\,m^{-3}$ ($+0.5 \pm 0.28\,\mathrm{ppbv}$), and $-0.02 \pm 0.01\,\mu g\,m^{-3}$ ($+4.3 \pm 0.33\,\mathrm{ppbv}$), respectively. Total changes in $PM_{2.5}$ are associated with 1.5 (95 % confidence interval, CI, 1.0–2.5) million all-cause mortalities annually and in O_3 are associated with 375 (95 % CI, 129–592) thousand respiratory mortalities annually. Most air pollution mortality is driven by changes in emissions of short-lived air pollutants and their precursors (95 % and 85 % of mortalities from $PM_{2.5}$ and O_3, respectively). However, changing climate and increasing CH_4 concentrations also increased premature mortality associated with air pollution globally up to 5 % and 15 %, respectively. In some regions, the contribution of climate change and increased CH_4 together are responsible for more than 20 % of the respiratory mortality associated with O_3 exposure. We find the interaction between

climate change and atmospheric chemistry has influenced atmospheric composition and human mortality associated with industrial air pollution. In addition to driving 13 % of the total historical changes in surface O_3 and 15 % of the associated mortalities, CH_4 is the dominant factor driving changes in atmospheric OH and H_2O_2 since preindustrial time. Our study highlights the benefits to air quality and human health of CH_4 mitigation as a component of future air pollution control policy.

1 Introduction

Human activities since preindustrial time have resulted in large increases in air pollution (IPCC, 2001). Measurements at various sites in the Northern Hemisphere indicate an increase from the 1860s to 2000s in surface ozone (O_3) of approximately a factor of 4 (from about 10 to 50 ppbv) (Gros, 2006; Marenco et al., 1994). Sulfate and carbonaceous aerosol concentrations in Greenland ice cores suggest a factor of 3–4 increase from the mid-1860s to the present (Döscher et al., 1995; Fischer et al., 1998; Lavanchy et al., 1999). Sulfate and carbonaceous aerosols are key components of fine particulate matter ($\leq 2.5\,\mu m$ aerodynamic diameter, $PM_{2.5}$) which, along with O_3, are pollutants that adversely impact human health (Jerrett et al., 2009; Krewski et al., 2009; Pope and Dockery, 2006; Levy et al., 2005; Bell et al., 2004; Pope et al., 2002). Here, we apply simulations of a global coupled chemistry-climate model to investigate changes in O_3 and $PM_{2.5}$ from the preindustrial era to the present and their associated effects on premature mortality.

O_3 is a secondary air pollutant that is formed in the troposphere by catalytic photochemical reactions of nitrogen oxides ($NO_x = NO + NO_2$) with carbon monoxide (CO), methane (CH_4) and other volatile organic compounds (VOCs). $PM_{2.5}$, including sulfate, nitrate, Organic Carbon (OC), Black Carbon (BC), secondary organic carbon, fine dust and sea salt, is either directly emitted from various sources or produced via chemical reactions between directly-emitted gas-phase precursors (including SO_2, NO_x, NH_3 biogenic VOCs etc.) and atmospheric oxidants (i.e., OH, H_2O_2, O_3). Changes in O_3

and PM$_{2.5}$ concentrations over this period (1860–2000) are difficult to quantify because of sparse and uncertain preindustrial measurements, spatial heterogeneity of these species, uncertainties in estimating preindustrial emissions, and the non-linear dependence of O$_3$ and PM$_{2.5}$ on their precursor emissions (Horowitz, 2006). Changes in surface O$_3$ and PM$_{2.5}$ concentrations are largely controlled by changes in emissions of their precursors. Consequently, many recent studies have applied Chemical Transport Models (CTMs) to estimate changes in tropospheric O$_3$ and aerosol concentrations from the preindustrial era to the present (Horowitz, 2006; Tsigaridis et al., 2006; Lamarque et al., 2005; Grenfell et al., 2001; Mickley et al., 2001; Wang and Jacob, 1998). Annenberg et al. (2010) used preindustrial and present simulations from one of these CTM modeling studies (Horowitz 2006) to estimate the effect of anthropogenic O$_3$ and PM$_{2.5}$ on present premature human mortality. However, these studies, which usually apply different emissions of short-lived species but use the same meteorological driver for preindustrial and present day simulations, do not take into account the interaction between climate and air pollution (Jacob and Winner, 2009; Isaksen et al., 2009; Fiore et al., 2012). Some short-lived species are radiatively active; therefore, they perturb climate and meteorology from regional to global scales (Naik et al., 2012; Levy et al., 2008; Shindell et al., 2008). As a result, quantifying the impact of their emission changes on air quality using CTM simulations driven by the same meteorology neglects the feedbacks between short-lived species and climate. Conversely, studies have shown that climate change can affect surface O$_3$ and PM$_{2.5}$ concentrations and thus indirectly affect human mortality (Fang et al., 2012; Tagaris et al., 2009; Bell et al., 2007). Additionally, methane (CH$_4$) concentration changes (from 800 ppbv in 1860 to 1750 ppbv in 2000) not only give a direct radiative forcing of $+0.42\,\mathrm{W\,m^{-2}}$ (calculated as in Ramaswamy et al., 2001), but also contribute to increasing O$_3$ concentrations. To understand changes in surface O$_3$ and PM$_{2.5}$ over the industrial period (defined here as 1860–2000), we need to consider the effects of changing emissions of short-lived species, climate and CH$_4$ concentrations on surface air quality and allow feedbacks between chemistry and climate to take place.

In this paper, we utilize the Geophysical Fluid Dynamics Laboratory (GFDL) Atmospheric Model, version 3 (AM3), a newly developed global 3-D model that fully couples atmospheric chemistry and climate. Our goal is to understand changes in O_3 and $PM_{2.5}$ from the preindustrial era to the present ("industrial" or "historic" period) and their associated effects on premature mortality. We further attribute the changing $PM_{2.5}$ and O_3 concentrations over this period to three factors: (1) changes in direct emissions of their constituents and precursors; (2) climate change induced changes in surface concentrations, and (3) the influence of increasing methane (CH_4) concentrations on tropospheric chemistry. For each factor we estimate the associated impact on human health. The GFDL AM3 model and our simulations are described in Sect. 2. We evaluate simulated surface O_3 and $PM_{2.5}$ concentrations in Sect. 3. Changes in surface air quality are attributed to specific factors in Sect. 4. In Sect. 5, we calculate the changes in premature mortality associated with the simulated changes in air quality. Findings and conclusions are presented in Sect. 6.

2 Methods

2.1 Model description

The AM3 model (Donner et al., 2011) is the atmospheric component of the GFDL atmosphere-ocean coupled climate model CM3. AM3 is designed to address key emerging issues in climate science, including aerosol-cloud interactions and chemistry-climate feedbacks. It is GFDL's first global atmospheric model to include the indirect effects of cloud-aerosol interactions (with 16 interactive aerosol species) and of tropospheric and stratospheric chemistry (with 81 gas species) coupled with climate. Detailed chemistry, emissions, and deposition processes in AM3 are described in Naik et al. (2012) with additional details described below, and transport (advection, vertical diffusion and convection) along with physics are described by Donner et al. (2011). The model uses a finite-volume dynamical core with a 6 × 48 × 48 cubed-sphere horizontal

grid with the grid size varying from 163 km (at the corners of each face) to 231 km (near the center of each face). Vertically, the model extends from the surface up to 0.01 hPa (86 km) with 48 vertical hybrid sigma pressure levels.

2.2 Simulations

To investigate the change in concentrations of O_3 and $PM_{2.5}$ during the "industrial period", we use AM3 timeslice simulations – "1860" and "2000". Results from these simulations were contributed to the Atmospheric Chemistry and Climate Model Intercomparison Project (ACCMIP) (Lamarque et al., 2012). To evaluate the relative importance of the drivers of air pollutant concentration changes: (1) anthropogenic and biomass burning emissions of short-lived air pollutants, (2) climate and (3) CH_4 concentration, we also analyze three additional sensitivity simulations. The five simulations used are summarized in Table 1 and described briefly below.

We use the "1860" and "2000" simulations to quantify the change in air quality during the "industrial period". These simulations use prescribed mean climatological Sea Surface Temperature (SST) and Sea Ice Cover (SIC) for the decade 1860–1869 and 1995–2004, respectively, taken from one member of the 5-member ensemble historical simulation of the GFDL CM3 model conducted in support of the Intergovernmental Panel on Climate Change-Fifth Assessment Report (IPCC-AR5). Well-mixed greenhouse gases (WMGG), including CO_2, N_2O, CH_4 and CFCs, are specified for the years 1860 and 2000 according to the database (http://www.iiasa.ac.at/web-apps/tnt/RcpDb/dsd?Action=htmlpage&page=welcome) developed in support of the IPCC-AR5 (Meinshausen et al., 2011). Global mean CH_4 concentration is specified at the surface at 1860 and 2000 levels, respectively, as lower boundary conditions for tropospheric chemistry calculations Anthropogenic emissions (including from energy production, industry, land transport, maritime transport, aviation, residential and commercial sectors, solvents, agriculture, agriculture waste burning on fields, and waste) and biomass burning emissions (including from open vegetation fires in forests, savanna and grasslands) of short-lived air pollutants (i.e., NO_x, CO, SO_2, NMVOCs, black carbon and

organic carbon, etc.) for 1860 and 2000 are from the emission inventory of Lamar-que et al. (2010). Anthropogenic emissions for 2000 were constructed by aggregat-ing existing regional and global emission inventories for 40 world regions and 10 sec-tors. Anthropogenic emissions for 1860 were generated based on extrapolation of the

EDGAR-HYDE emission inventory from 1890 to 1850 using global fossil fuel consump-tion estimates from Andres et al. (1999) and regional scale data for population from the HYDE dataset (Goldewijk, 2005). Biomass burning emissions in 2000 are from the GFED2 emission inventory (van der Werf et al., 2006); the 1900–2000 biomass burn-ing emission trend is taken from RETRO (1960–2000, Schultz et al., 2008) and GICC

(1900–1950, Mieville et al., 2010) inventories; no trend is assumed between 1850 and 1900 as suggested by ice-core and charcoal records (Marlon et al., 2008; McConnell et al., 2007). The 1860 and 2000 anthropogenic and biomass burning emissions used are summarized in Table S1 of the Supplement. As described by Naik et al. (2012), all natural emissions except those that depend on the simulated meteorology (lightning

NO_x dimethyl sulfide (DMS), sea salt and dust emissions), are the same for both sim-ulations. Ozone depleting substances (ODS) are set to pre-1950 levels in the "1860" simulation and to 2000 levels in the "2000" simulation. All simulations were run for 11 yr with the first year used as spin up.

We define the difference in $PM_{2.5}$ and O_3 concentrations between the AM3 "2000"

and "1860" simulations as "industrial" air pollution, which reflects the total changes in air pollution levels between the start of the industrial period and 2000. Our definition of "industrial" pollution includes not only the effect of changes in short-lived air pollutant emissions, but also the effect of changes in climate, CH_4 and ODS concentrations. It differs from the "anthropogenic" pollution defined in Anenberg et al. (2010), which was

estimated as the difference between two CTM simulations with different emissions and, therefore, solely reflected the impact of emission changes on air pollution in a system that did not allow feedbacks between chemistry and climate.

To isolate the individual impacts of changes in emissions, climate, and CH_4 concen-trations on surface concentrations of O_3 and $PM_{2.5}$, we analyze three additional AM3

Full Screen / Esc

Printer-friendly Version

Interactive Discussion

simulations (simulations 3, 4 and 5 in Table 1). Briefly, simulation "2000CL1860EM" is similar to the "2000" simulation but uses 1860 emissions of short-lived species; simulation "1860CL2000EM" is also similar to the "2000" simulation but its' SST, SIC, WMGG and ODS concentrations (applied in stratospheric chemistry and radiative forcing calculations) are set to 1860 levels; simulation "1860ALL2000EM" is similar to "1860CL2000EM", but its global mean CH_4 concentration is also specified at 1860 levels for tropospheric chemistry calculations. Impacts of (1) changing emissions of short-lived species, (2) changing climate and (3) changing CH_4 concentrations on air quality are estimated in our study as "2000"-"2000CL1860EM", "2000"-"1860CL2000EM", and "1860CL2000EM"-"1860ALL2000EM", respectively. In order to distinguish signals driven by changing emissions, CH_4 and climate from internal model variability, we use annually-invariant SST, SIC and air pollutant emissions to drive 10-yr model simulations and analyze averages of these 10-yr simulations. To indicate the significance of a result relative to the inter-annual variability due to internal model variability, we report a mean (average of all 10 yr) along with the standard deviation (root mean square of variance over the 10 yr) in the following sections (as mean ± std).

2.3 Adverse health impacts

We analyze the effect of industrial air pollution on premature mortality using health impact functions that relate changes in air pollutant concentrations to changes in mortality. We further evaluate the relative importance of changes in emissions of air pollutants, climate change and increased CH_4 concentrations on the incidence of premature mortalities associated with air pollution.

To obtain estimates of the excess mortalities (ΔMort) attributable to air pollution changes during the industrial period we use health impact functions for O_3 and $PM_{2.5}$. These functions are based on log-linear relationships between relative risk and concentration derived from American Cancer Society (ACS) cohort studies for adults aged

30 and older (Jerrett et al., 2009; Krewski et al., 2009; Pope et al., 2002). We apply

$$\Delta \text{Mort} = \text{POP} \times \text{Frac} \times \text{Mort}_{\text{base}} \times (1 - e^{-\beta \Delta C}) \qquad (1)$$

in each of the AM3 surface grid cells using the corresponding population (POP), base-line mortality (Mort$_{\text{base}}$), and consistent with the ACS study, the fraction of the population (Frac) $\geq$ 30 yr of age and the appropriate concentration-mortality response factor (β). Changes in O_3 and $PM_{2.5}$ concentrations (ΔC) from specific factors (changes in short-lived emissions, climate and CH_4) from preindustrial to present day are obtained as the exposure indicators from the difference between two simulations as described in Sect. 2.2, consistent with corresponding epidemiological studies. Table 2 summarizes the epidemiological studies and their β values that are applied in our study. We use population (CIESIN, 2005), population fraction of adults aged 30 and older (WHO, 2003) and baseline mortality for the year 2000 for all-cause mortality and for respiratory mortality (WHO, 2003) as in Fang et al. (2012). For $PM_{2.5}$, although relative risk values for ischemic heart disease (a subset of cardiopulmonary disease) is reported and is used by Anenberg et al. (2010), we choose to use β for all-cause mortality as reporting of total mortality in developing countries is likely more reliable than attribution of death to specific diseases. We assume the ACS cohort studies conducted in the United States are valid globally, as relative risks characterized in US based time series studies are similar to those found in various studies in Europe (Levy et al., 2005) and Asia (HEI, 2010) and no cohort studies have yet been conducted in developing countries However, we recognize that there exist differences in $PM_{2.5}$ composition, health status, lifestyle, age structure, and medical attention available around the world, which could significantly affect our results

3 Model evaluation

Various simulated physical and chemical parameters in AM3 have been evaluated by Donner et al. (2011) and Naik et al. (2012). Here we evaluate the ability of our "2000"

AM3 simulation to reproduce observed surface O_3 and $PM_{2.5}$ concentrations around the world in order to increase confidence in our estimates of the excess mortalities attributable to air pollution.

We evaluate surface O_3 in our 2000 simulation against surface O_3 data from observational networks in the United States (Clean Air Status and Trends Network-CASTNet) and in Europe (European Monitoring and Evaluation Programme-EMEP). Sites in these two networks are well-suited for evaluating global models as they represent regional O_3 concentrations rather than urban plumes. A comparison between the simulated and observed seasonal cycle of O_3 over twelve regions spanning the US and Europe is shown in Fig. 1. In general, like in Naik et al. (2012), the AM3 "2000" simulation reproduces the observed seasonal cycle of surface O_3 concentrations over most regions ($r > 0.7$ and bias < 20 ppbv, except in the Northwest United States). Naik et al. (2012) attribute the strong positive bias of O_3 in the Northwest U.S. to the model failure to capture the influence of maritime air masses on sites close to the ocean. However, over populated areas, such as the Eastern United States, South California and Europe, surface O_3 bias is relatively small (ranging from 4 ppbv to about 10 ppbv) and the simulated O_3 seasonal cycle follows observed cycles with correlation coefficients greater than 0.7. Correlation coefficients are greater than 0.95 over all 6 European regions.

The optical characteristics of aerosols simulated in AM3 were evaluated by Donner et al. (2011), who found that simulated AOD was within a factor of 2 of AERONET observations. However, annual mean surface $PM_{2.5}$ mass concentration simulated by AM3, which is directly associated with human mortality responses, has not yet been evaluated. Here, we evaluate annual mean $PM_{2.5}$ concentrations (or its major component, sulfate, where long-term $PM_{2.5}$ observations are not available) for the 2000 simulation with observations over the United States (the U.S. Air Quality System, US-AQS), Europe (EMEP) and East Asia (Acid Deposition Monitoring Network in East Asia, EANET). Measured concentrations are averaged over corresponding model grids for 1997–2003 and 1995–2004 for the USAQS ($PM_{2.5}$) and EMEP (sulfate) datasets, respectively. Asian sulfate observations are collected from Liu et al. (2009) and Zhang

Air pollution and associated human mortality

Y. Fang et al.

et al. (2011). Figure 2 shows a consistent underestimate of total $PM_{2.5}$ over the United States. However, the bias for dust (Ginoux, in prep.) and sulfate over Europe and East Asia is much smaller (Fig. 2a). The greater underestimate of total $PM_{2.5}$ than dust or sulfate in the AM3 2000 simulation is likely related to the simulation of secondary or-
5 ganic aerosol (SOA). AM3 SOA production is scaled directly from terpene emissions and butane oxidation (Donner et al., 2011); therefore, it may underestimate SOA away from terpene and butane sources. Additionally, AM3 does not consider SOA produced by oxidation of isoprene and does not include in-cloud mechanisms for SOA production and thus likely underestimates total SOA production. Despite the systematic $PM_{2.5}$
10 underestimate of more than 20 %, AM3 captures the global spatial distribution of $PM_{2.5}$ well, with a correlation coefficient above 0.9.

4 Surface $PM_{2.5}$ and O_3 concentration changes

We first quantify the increase in surface concentrations of $PM_{2.5}$ and O_3 due to "industrial pollution" from preindustrial time (year 1860) to the present (year 2000) (TOTAL)
15 in Sect. 4.1. In the following subsections, we analyze the causes of these changes and attribute them to three factors: changes in emissions of air pollutants (EMIS, Sect. 4.2), climate, (CLIM, Sect. 4.3) and CH_4 concentrations (TCH4, Sect. 4.4). As atmospheric OH and H_2O_2 control the gas- and aqueous-phase production of major $PM_{2.5}$ components (such as sulfate) and are important for explaining $PM_{2.5}$ changes especially when
20 discussing CH_4 effects, we also examine changes in their concentrations throughout this section.

4.1 Total changes from 1860 to 2000

Distributions of annual mean surface $PM_{2.5}$ and health-relevant O_3 (defined as the maximum 6-month mean of 1-h daily maximum O_3 in a year, denoted as H-O_3) in
25 year 2000 are shown in Figs. 3a and 3b. Global population-weighted concentrations

of $PM_{2.5}$ and $H-O_3$ are $13 \pm 0.15\,\mu g\,m^{-3}$ and $61 \pm 0.20\,ppbv$ (Table 3). Both $PM_{2.5}$ and $H-O_3$ show maximum concentrations close to source regions in East Asia, Eastern United States, India and Central Africa. High concentrations of $PM_{2.5}$ (ranging from 20 to $40\,\mu g\,m^{-3}$) over Northern Africa and the Middle East are associated with strong dust emissions. Present-day tropospheric air mass-weighted OH and H_2O_2 concentrations are $1.19 \pm 0.01 \times 10^6$ and $1.95 \pm 0.01 \times 10^{10}$ molec cm^{-3}. The global mean OH concentration in the "2000" simulation is consistent with the climatological mean of Spivakovsky et al. (2000).

Total changes in $PM_{2.5}$ and $H-O_3$ from preindustrial to present ("2000"–"1860"), shown in Figs. 3c and 3d, reflect changes in pollutant concentrations resulting from changes in all factors between 1860 and 2000 (TOTAL). During industrialization, concentrations of air pollution increased over most regions, particularly over populated areas in the Northern Hemisphere. Global population-weighted annual mean $PM_{2.5}$ and $H-O_3$ increased from 1860 to 2000 by $8 \pm 0.16\,\mu g\,m^{-3}$ and $30 \pm 0.16\,ppbv$, respectively (Table 3). Because of the coincidence of large concentration increases and densely populated areas, population-weighted global mean concentration changes are substantially higher than their land-only area-weighted mean values ($3 \pm 0.10\,\mu g\,m^{-3}$ and $20 \pm 0.12\,ppbv$). Increases in $PM_{2.5}$ and O_3 during the industrial period account for 61% and 49%, respectively, of their year 2000 concentrations.

Our simulated population-weighted changes in $PM_{2.5}$ and O_3 from 1860 to 2000 are smaller than those reported in Anenberg et al. (2010) ($15.0\,\mu g\,m^{-3}$ and $37.1\,ppbv$), in large part due to the use of different present and preindustrial emissions in the two studies. Different from the emission inventory we use (Sect. 2.2), the 2000 emissions of Anenberg et al. (2010) were obtained by scaling their standard 1990 emissions (taken from EDGAR v2.0) by the 2000 to 1990 ratio of SRES emissions (Nakicenovic et al., 2000) in four geopolitical regions (Horowitz, 2006). Their preindustrial fossil fuel emissions are assumed to be zero, while their preindustrial emissions from burning of biofuels, savannah, tropical forest and agricultural waste are assumed to be 10% of their standard 1990 emissions. Preindustrial emissions of NO_x, CO, BC and OC in

Anenberg et al. (2010) are all lower than in this study (see Supplement, table S2). Differences in 2000 emissions are generally larger than differences in the 1860 emissions of the two inventories. The resulting differences in emissions between the two studies are large. For example, the historical increase in SO_2 emissions in this study and in Anenberg et al. (2010) is 100 and 150 Tg per year, respectively; BC emission changes differ by even more, 4.4 vs.10 Tg C per year, respectively; differences in NO_x emission changes are 31.7 vs. 35.0 Tg N per year. The greater emission changes from 1860 to 2000 in Anenberg et al. (2010) than in our study drive their higher estimate of changes in surface $PM_{2.5}$ and O_3. We chose our emission inventory because it is newly developed to capture the best current information. It is widely used in various climate (and chemistry-climate) models in support for the IPCC AR5 report and the Atmospheric Chemistry and Climate Model Inter-comparison Project (ACCMIP) (Lamarque et al., 2012, 2010). Finally, in addition to differences in emission inventories, our study intrinsically differs from Anenberg et al. (2010) as changes in $PM_{2.5}$ and O_3 from 1860–2000 here result from changes in climate, ODS and CH_4 as well as from emission changes.

From preindustrial time to present day, simulated tropospheric air mass-weighted OH and H_2O_2 concentrations change by $-0.11 \pm 0.01 \times 10^6$ and $+0.84 \pm 0.01 \times 10^{10}$ molec cm^{-3}, approximately -8% and $+75\%$ relative to their 1860 levels. The simulated decrease in OH and increase in H_2O_2 concentrations from the preindustrial to present period are consistent with observational records from Greenland ice cores and permafrost, respectively (Sigg and Neftel, 1991; Staffelbach et al., 1991). Changes in OH concentrations are also within the range of estimates in the literature (Naik et al., 2012; John et al., 2012).

In the following subsections, we separately explore the role of historical changes in emissions of short-lived species, climate and CH_4 on surface $PM_{2.5}$, O_3, and atmospheric OH and H_2O_2, using sensitivity simulations introduced in Sect. 2.2.

4.2 Impact of changes in emissions of short-lived species

Here we quantify how historical changes in short-lived species emissions affect surface air quality by comparing the "2000" simulation with a simulation with 2000 climate (SST, SIC and WMGG) but 1860 emissions of short-lived species ("2000CL1860EM"). Global CH$_4$ concentrations applied as the lower boundary condition for tropospheric chemistry calculations are specified at 2000 levels in both simulations. The same simulations have been analyzed by Naik et al. (2012) to evaluate the effect of increased emissions of short-lived species on tropospheric composition and climate forcing. In contrast, we analyze changes in surface PM$_{2.5}$ and O$_3$, two species of major concern to public health.

Distributions of surface PM$_{2.5}$ and H-O$_3$ changes resulting from changes in short-lived air pollutant emissions are shown in Figs. 3e and 3f ("2000" - "2000CL1860EM"). Changing emissions raises the global annual mean population-weighted concentration of PM$_{2.5}$ by $7.5 \pm 0.19\,\mu g\,m^{-3}$ (Table 3), accounting for 94 % of the total change in PM$_{2.5}$ from 1860 to 2000. The PM$_{2.5}$ pattern resulting from changes in short-lived pollutant emissions (Figure 3e) is strongly correlated ($R = 0.99$) with the pattern of the total changes resulting from all three factors between 1860 and 2000 (Fig. 3c).

Emission changes applied in this study include both anthropogenic and biomass burning emissions, both of which were influenced by human activity during the industrial period. Anthropogenic emissions increase during the industrial period almost everywhere while changes in biomass burning emissions driven by human activities are spatially inhomogeneous. For example, from 1860 to 2000, sulfate concentrations increase everywhere, especially in the Northern Hemisphere mid-latitudes, driven by enhanced anthropogenic precursor emissions (a factor of 18 increase in sulfur dioxide emissions, Table 2 in Naik et al., 2012). However, BC and OC decrease over the U.S. while increasing over Central Africa and tropical South America. This is driven by less biomass burning in the United States and more in the tropics in 2000 than in 1860 (Fig. 6 in Naik et al., 2012). According to Mieville et al. (2010), in boreal regions, burnt

Title Page

Abstract | Introduction

Conclusions | References

Tables | Figures

◄ | ►

◄ | ►

Back | Close

Full Screen / Esc

Printer-friendly Version

Interactive Discussion

surface area and biomass burning emissions have decreased over the past one to two centuries as a result of human-induced land-use change and fire suppression policy. In contrast, over Central Africa, Central South America and Indonesia, biomass burning emissions have increased over the past few decades due to human pressure and to the use of fire for deforestation as part of agriculture expansion (Mieville et al., 2010).

Naik et al. (2012) found that increases in O_3 precursor emissions from preindustrial time to the present lead to 45 % and 40 % increases in the photochemical production and loss of O_3, respectively, leading to a 21 % increase in tropospheric O_3 burden. As a result, the global mean population-weighted H-O_3 increases by 25 ± 0.30 pbbv (Table 3). Although the distribution of emission-driven changes in H-O_3 (Fig. 3f) correlates well with that of the total change in H-O_3 from 1860 to 2000 (Fig. 3d, $R = 0.99$), the emission-driven increase of H-O_3 accounts for only 83 % of the total increase (30 ± 0.16 ppbv), indicating that other factors also influence changes in H-O_3 concentrations. We show in Sects. 4.3 and 4.4 that changing climate and increased CH_4 concentrations drive the rest of the H-O_3 increase.

OH and H_2O_2 concentrations are also affected by increases in emissions of short-lived species. Tropospheric air mass-weighted OH and H_2O_2 concentrations increase from 1860 to 2000 by $+0.13 \pm 0.01 \times 10^6$ and $+0.41 \pm 0.02 \times 10^{10}$ molec cm^{-3} due to changes in short-lived emissions alone, about +10 % and +37 % relative to their 1860 values, respectively. Increases of OH and H_2O_2, combined with higher SO_2 emissions, further increase sulfate production. However these short-lived species emission-driven changes are substantially different from the total changes in OH and H_2O_2 ($-0.11 \pm 0.01 \times 10^6$ and $+0.84 \pm 0.01 \times 10^{10}$ molec cm^{-3}), indicating that other factors strongly influence their concentrations as shown in the following subsections. Due to increases in emissions of short-lived species, aerosols become more abundant in the atmosphere and are associated with decreased precipitation in the AM3 model (Naik et al., 2012; Donner et al., 2011). In our study, due to feedbacks resulting from increases in emissions of short-lived species, global precipitation decreases by 0.03 mm day^{-1} with significant large decreases (about 1mm day^{-1}) over

source regions, such as East Asia; and as a result, sulfate lifetime to wet deposition increases from 6.4 days in 1860 to 6.9 days in 2000. Increases in emissions of short-lived species also cause a net negative all-sky radiative forcing ($-1.43\,\mathrm{W\,m^{-2}}$) (Naik et al., 2012), cooling the atmosphere and reducing chemical reaction rates (although this effect varies locally depending on the location and type of aerosols). Our study using AM3 captures these chemistry-climate feedback processes associated with changes in aerosol/trace gas abundance in the atmosphere and goes beyond previous CTM studies that investigate the impact of historical emission changes on atmospheric composition (Horowitz, 2006; Lamarque et al., 2005).

4.3 Impact of historical climate change

Historical climate change indirectly affects surface $PM_{2.5}$ and O_3 by modifying transport patterns, precipitation, water vapor, and temperature-dependent reaction rates. Here we estimate the effect of historical climate change on surface $PM_{2.5}$ and O_3 by comparing the "2000" simulation with short-lived species emissions set at 2000 levels but with year 1860 SST, SIC and WMGG ("1860CL2000EM"). The global CH_4 concentration applied as the lower boundary condition for tropospheric chemistry calculations is set to 2000 levels in both simulations so that we can isolate the role of climate change on air quality rather than the impact of CH_4 on tropospheric chemistry. The two simulations analyzed here have different ODS concentrations (Table 1), therefore, the impact of historical climate change also includes the effects of stratospheric O_3 depletion caused by anthropogenic ODS emissions over this period. However, our historical climate change does not include the climate change induced effect on biogenic emissions of air pollutant precursors, such as isoprene and terpenes. If a biogenic response to the changing climate were included, it would likely increase our estimate of changes in $PM_{2.5}$ and O_3 concentrations described below.

4.3.1 PM$_{2.5}$

From 1860 to 2000, our simulation indicates that climate change caused global population-weighted PM$_{2.5}$ concentrations to increase by $0.4 \pm 0.17\,\mu g\,m^{-3}$ (Table 3), accounting for 5 % of the total increase over this period. The spatial distribution of PM$_{2.5}$ changes, driven by climate change and driven by all factors, is only loosely corre-lated ($R = 0.3$). Changes in PM$_{2.5}$ driven by climate change show a complicated pattern (Fig. 3g): modest increases (up to $2\,\mu g\,m^{-3}$) occur over East Asia, South and South-East Asia, West Africa and Central Europe; significant decreases (up to $1.5\,\mu g\,m^{-3}$) occur over the United States, Central Asia, and Central and Western Australia. Signifi-cant decreases over Central and Western Australia are driven by lower concentrations of sea salt and dust (not shown), two PM$_{2.5}$ components with emissions dependent on meteorology. Increases that are statistically significant over Asia, India and Central Europe are driven by increases in BC, sulfate and OC, with OC accounting for a ma-jority of the enhanced PM$_{2.5}$. Increases in the concentration of these species is driven by reductions in large-scale precipitation, the major driver of wet deposition (Fig. 4). Increases also result from higher H$_2$O$_2$ concentrations (discussed below) that increase the aqueous phase production of sulfate. Decreases in PM$_{2.5}$ over the United States and Central Asia are driven by stronger large-scale precipitation/wet deposition close to their PM$_{2.5}$ precursor source regions (Fig. 4). While changes in PM$_{2.5}$ driven by climate change are statistically significant over most continental regions, 10-yr simulations are likely too short to generate a robust signal for precipitation distinguishable from noise on a regional scale (Naik et al., 2012). Figure 4 shows that simulated differences in large-scale precipitation is significant at the 95 % confidence level over part of East Asia, North India and Central Europe and many ocean regions, but is not significant elsewhere. If we lower the confidence level to 90 %, regions with statistically signifi-cant differences in precipitation become larger over Asia and India (see Supplement, Fig. S1).

Full Screen / Esc

Printer-friendly Version

Interactive Discussion

4.3.2 Ozone

As a result of historical climate change and stratospheric O_3 depletion, the global population-weighted H-O_3 concentration increases by 0.5 ± 0.28 ppbv (Table 3), accounting for less than 2 % of the total historical H-O_3 change. Despite the small contribution, the spatial distribution of H-O_3 changes driven by climate change follows that driven by all factors with a correlation coefficient of 0.71. Historical climate change leads to increases in O_3 over polluted areas and at high-latitudes in the Northern Hemisphere, while decreasing O_3 over remote regions and oceans (Fig. 3h). This pattern, similar to that of surface O_3 responses to a warming climate in the future (Fang et al., 2012; Liao et al., 2006; Murazaki and Hess, 2006), is mainly associated with the tropospheric chemistry of O_3 under a warmer and wetter atmosphere. O_3 decreases over remote oceanic regions is largely driven by an increase in water vapor (total column water vapor increases by 3 % from preindustrial times), which leads to increases in HO_x ($HO_x = OH + HO_2$) concentrations ($+3.6 \pm 0.1 \times 10^6$ molec cm^{-3}). Reaction with HO_x is the primary sink of O_3 at low NO_x concentrations. However, surface O_3 increases by up to 3 ppbv over regions with large NO_x emissions such as South China, North India, Northeast United States, Central Europe and Central Africa. Factors contributing to increases over these regions include: (1) increased O_3 production due to higher water vapor leading to more abundant HO_x; (2) warmer global average temperature ($+0.5°$) from 1860 to 2000, increases photochemistry rates and decreases net formation of peroxyacetyl nitrate (PAN, $CH_3C(O)OONO_2$), a reservoir species for NO_x, leaving more NO_x available over source regions and promoting local O_3 production; and (3) increased lightning that increases production of lightning NO_x ($+3$ %). While lightning NO_x is mostly formed in the free troposphere and contributes to stronger tropospheric O_3 production, its contribution to surface O_3 is small, most likely over regions where subsidence brings lightning-affected air masses to the surface, such as the Southwestern United States (Fang et al., 2010).

During this historical period, anthropogenic emissions of ODS caused stratospheric O_3 depletion. Stratospheric O_3 depletion and the associated changes in J-values in the troposphere, combined with changes in transport between stratosphere and troposphere, also affect tropospheric O_3. To estimate this effect on surface O_3, we first evaluate changes in the cross-tropopause O_3 fluxes, and find the net flux decreases by almost 15 % relative to its level in the 1860 simulation. To estimate the stratospheric O_3 contribution to surface O_3, we further analyze an additional tracer of stratospheric O_3 implemented in these simulations (O_{3S}). This tracer, as described in Lin et al. (2012), is defined as O_3 above the World Meteorological Organization (WMO) thermal tropopause at each model time step. Once mixed into tropospheric air, O_{3S} is subject to the same transport and loss as tropospheric O_3. Surface O_{3S} shows an annual global mean reduction of 0.7 ppbv, resulting from both stronger O_3 destruction and stratospheric O_3 depletion. Surface O_{3S} change has distinctive seasonal variations, with smaller decreases (−0.2 ppbv) in winter than in summer (−1.3 ppbv), consistent with projections that stratospheric-tropospheric exchange of O_3 increases in winter months in a warming climate (Liao et al., 2006; Collins et al., 2003; Zeng and Pyle, 2003). The decrease in O_{3S} concentration at the surface suggests that historical changes in stratospheric O_3 tend to decrease surface O_3 concentrations. However, this surface O_{3S} change likely overestimates changes in the stratospheric contribution to surface O_3 since any O_3 above the thermal tropopause is instantly labeled as "stratospheric" regardless of its actual origin (Lin et al., 2012).

4.3.3 H_2O_2 and OH

We find climate change drives changes in tropospheric air mass-weighted OH and H_2O_2 concentrations by $-0.02 \pm 0.01 \times 10^6$ and $+0.15 \pm 0.03 \times 10^{10}$ molec cm^{-3} (Table 3). The change in OH is small, reflecting competing effects between increases in tropospheric NO_x (due to stronger lightning sources), SO_2 (due to weaker wet deposition) and water vapor (due to higher temperature), and decreases in O_3 burden. The

increase in H_2O_2 suggests enhanced conversion of HO_2 to H_2O_2 rather than cycling back to OH.

4.4 Impact of increased CH_4 concentration

The simulated change in H-O_3 and $PM_{2.5}$ due to climate change explored in Sect. 4.2 does not allow changes in CH_4 concentration to affect tropospheric chemistry (Table 1). Although this configuration intentionally isolates the role of climate change, increases in CH_4 concentrations from 1860 to 2000 also affect tropospheric chemistry and hence surface O_3 and $PM_{2.5}$ concentrations. We estimate the effect of increased CH_4 concentrations on O_3 and $PM_{2.5}$ concentrations by taking the difference between the "1860CL2000EM" and "1860ALL2000EM" simulations (Figs. 3i and 3j). Both simulations are identical except that the global mean CH_4 concentrations applied in the tropospheric chemistry calculations are set to year 2000 (1750 ppbv) and 1860 (800 ppbv) levels, respectively.

Tropospheric CH_4 perturbs the concentrations of oxidizing agents in the atmosphere, which in turn affect $PM_{2.5}$ and O_3 concentrations. In addition, CH_4 is a precursor of tropospheric ozone. Reaction with CH_4 is a primary sink of atmospheric OH. Higher CH_4 concentrations in 2000 than 1860 result in an OH decrease of $0.24 \pm 0.01 \times 10^6$ molec cm^{-3} and an increase of $0.35 \pm 0.03 \times 10^{10}$ molec cm^{-3} in H_2O_2 (Table 3). As OH and H_2O_2 are associated with the gas-phase and in-cloud production of sulfate, changing CH_4 thus indirectly influences $PM_{2.5}$. Compensating changes in OH and H_2O_2 lead to a small and insignificant global change in $PM_{2.5}$ (global population-weighted $PM_{2.5}$ decreases by $0.04 \pm 0.24\,\mu g\,m^{-3}$, Table 3). The spatial pattern of $PM_{2.5}$ changes driven by the impact of increased CH_4 concentration is also not correlated with its total change during the industrial period.

CH_4 increases (from 800 ppbv in 1860 to 1750 ppbv in 2000) result in an increase in the global population-weighted H-O_3 concentration of 4.3 ± 0.33 ppbv (Table 3, TCH4), accounting for almost 15 % of the total H-O_3 produced during the industrial period. The

distribution of surface O_3 enhancement driven by increased CH_4 is significant everywhere in the world and is approximately 5–10 ppbv in the Northern Hemisphere and 2–5 ppbv in the Southern Hemisphere (Fig. 3j). A spatial correlation of 0.7 between changes in surface H-O_3 driven by increased CH_4 and that driven by all factors supports total O_3 changes being partly driven by CH_4. Although the impact of CH_4 on O_3 has been discussed in previous literature (Fiore et al., 2008, 2002; West et al., 2006; Dentener et al., 2005), most recent studies focus on exploring the potential benefit of future CH_4 mitigation while our study examines the total change in O_3 resulting from historic increases in CH_4. Fiore et al. (2008), however, estimated that anthropogenic CH_4 contributes 5 ppbv to global mean surface O_3 which, despite differences in approach, is consistent with our result of a 4.3 ppbv increase in H-O_3.

5 Premature mortalities associated with industrial air pollution

5.1 Estimate of premature mortalities associated with industrial air pollution

We estimate excess mortalities attributable to industrial air pollution separately for O_3 and $PM_{2.5}$, using population and baseline mortality rates at present (2000) along with concentration changes in O_3 and $PM_{2.5}$ from 1860 to 2000. Globally, in 2000, industrial $PM_{2.5}$ is associated with 1.52 (95 % confidence interval, CI, of 1.03–1.98) million all-cause mortalities per year (Table 4); while industrial O_3 is associated with 0.37 (95 % CI, 0.13–0.59) million respiratory mortalities per year (Table 4). Our estimates suggest that about 1.5 million all-cause premature mortalities and about 0.4 million respiratory mortalities would have been avoided in 2000 if surface $PM_{2.5}$ and O_3 had remained at 1860 levels (i.e., anthropogenic and biomass burning emissions of air pollution, CH_4 and climate had all remained the same in 2000 as they were in 1860). If we apply a low concentration threshold (LCT) of 5.8 $\mu g\,m^{-3}$ and 33.3 ppbv (the lowest values in the ACS studies), premature mortalities associated with industrial $PM_{2.5}$ and O_3 are 15 % and 11 % lower, respectively. These relative differences are smaller here than

in Anenberg et al. (2010) (33 % and 28 %, respectively for mortalities associated with $PM_{2.5}$ and O_3) because our preindustrial emissions and hence simulated preindustrial O_3 and $PM_{2.5}$ are higher than theirs (see Sect. 4 and Table S1). As differences with and without use of the LCT are relatively small in our study, we hereafter only report mortalities without the LCT.

We separate the world into 10 regions to estimate the regional mortalities associated with industrial air pollution. The distribution of premature mortality associated with industrial $PM_{2.5}$ and O_3 is shown in Figs. 5a and 5b. Eastern China and Northern India are hotspots for air pollution mortalities, driven by their large increases in surface $PM_{2.5}$ and O_3 concentrations and their large populations. East Asia (South Asia) account for 40 % (28 %) of the global all-cause mortalities associated with industrial $PM_{2.5}$ and 50 % (19 %) of the global respiratory mortalities associated with industrial O_3. None of the other regions contribute over 10 % to the global mortalities associated with industrial air pollution. North America and Europe account for a smaller fraction of global industrial $PM_{2.5}$ mortality (2 % and 5 %, respectively) than of global industrial O_3 mortality (7 % and 8 %, respectively) while Africa has the reverse results (7 % vs. 5 %).

5.2 Attribution of premature mortalities associated with industrial air pollution

In Sect. 4, changes in surface O_3 and $PM_{2.5}$ from preindustrial to present (2000) are attributed to changes in air pollutant emissions, climate and CH_4 concentrations. Here, we estimate the mortality responses using Eq. (1) with concentration changes driven by each factor separately.

5.2.1 Impact of changes in emissions of short-lived species

We estimate the global mortality response associated with industrial $PM_{2.5}$ and O_3 pollution resulting from changes in air pollutant emissions only ("2000"-"2000CL1860EM"). We find that if air pollutant emissions in year 2000 had remained at 1860 levels, 1.48 (95 % CI, 1.01–1.93) million all-cause mortalities associated with $PM_{2.5}$ exposure and

0.33 (95 % CI, 113–522) million respiratory mortalities associated with O_3 exposure could have been avoided.

5.2.2 Impact of historical climate change

We next estimate the global mortality response associated with industrial $PM_{2.5}$ and O_3 pollution resulting from climate change (and stratospheric O_3 depletion) ("2000" - "1860CL2000EM"). We find that if climate and stratospheric O_3 in 2000 were the same as in 1860, about 86 (95 % CI, 58–114) thousand all-cause mortalities associated with $PM_{2.5}$ exposure and 7 (95 % CI, 2–12) thousand respiratory mortalities associated with O_3 exposure could have been avoided.

5.2.3 Impact of increased global methane

Finally, we evaluate the effects of CH_4 concentration increases on global premature mortalities associated with air pollution. To be entirely consistent with the previous comparisons, we would compare $PM_{2.5}$ and O_3 in "2000" with that in a simulation identical to "2000" except with the lower boundary condition of global CH_4 concentration specified at 1860 instead of 2000 levels in its tropospheric chemistry calculation. Unfortunately, such a simulation is not available. However, two of our available simulations ("1860CL2000EM" and "1860ALL2000EM") although simulating 1860 climate, differ only in their treatments of CH_4 in tropospheric chemistry. This allows us to estimate the effect of increased CH_4 on premature mortality due to O_3 and $PM_{2.5}$ exposure We assume the bias due to the difference between 1860 and 2000 climates is small. Our results suggest that if CH_4 had remained at 1860 levels, about 50 (95 % CI, 17–82) thousand respiratory mortalities would have been avoided due to lower O_3 concentrations resulting from less CH_4.

5.2.4 Comparison of factors contributing to premature mortality

We further compare the mortality response associated with each factor (emission, climate and CH_4, see Figs. 5c–h) with total mortality associated with changes in industrial pollution regionally and globally to provide an approximation of the relative contribution of each factor to total air pollution mortalities in 2000 (the number of mortalities in each region due to each factor is summarized in Table S3 of the Supplement). For each region (i), we obtain a Normalized Mortality Contribution (NMC) in the following way:

$$\mathrm{NMC}_i = \frac{\text{Mortality responses driven by one anthropogenic factor}}{\text{Mortality responses driven by all anthropogenic factors}} \qquad (2)$$

Figure 6 shows NMC for each region. Due to the non-linearity in the health impact function, chemistry, and chemistry-climate system, the value of each bar in Fig. 6 is close to, but not exactly 1.

Global premature mortality associated with industrial $PM_{2.5}$, is dominated by increased emissions of reactive air pollutants ($\sim 95\%$), however, climate change is influential, contributing a global NMC of 5%. Regionally, contributions of climate change to total premature mortality associated with industrial $PM_{2.5}$ can be as high as 12% with the highest values over Europe and Australia. The impact of increased CH_4 concentrations on $PM_{2.5}$ and associated premature mortality globally is insignificant (Table 3).

The global premature respiratory mortality associated with industrial O_3 is also dominated by increased emissions of short-lived air pollutants (more than 85%). However increases in CH_4 are also influential, contributing a global NMC of 13% while the contribution of climate change is small with a global NMC of about 1%. On a regional scale, NMC of increased CH_4 ranges from 10 to 33% with the largest increases in excess mortalities in regions where increases in short-lived air pollutant emissions are relatively low (i.e., Australia, South America and Africa). Thus respiratory mortalities from industrial O_3 over relatively clean regions are more affected by rising global background CH_4 concentrations than other regions.

6 Discussion and conclusions

In this study, we apply the GFDL Atmospheric Model version 3 (AM3), a chemistry-climate model, to examine changes in surface O_3 and $PM_{2.5}$ from the preindustrial period to the end of the 20th century and associated changes in premature mortality. Simulated global population-weighted $PM_{2.5}$ and H-O_3 (health-related O_3, defined as the maximum 6-month mean of 1-h daily maximum O_3 in a year) concentrations increase by $8 \pm 0.16\,\mu g\,m^{-3}$ and $30 \pm 0.16\,ppbv$, respectively, from the preindustrial period to present-day (1860 to 2000). We quantify excess mortalities attributable to industrial air pollution and find that around year 2000, industrial $PM_{2.5}$ and O_3 are associated with 1.5 (95 % CI, 1.0–2.0) million annual all-cause mortalities and 0.37 (95 % CI, 0.13–0.59) million annual respiratory mortalities, respectively. India and China suffer most from industrial air pollution mortality as they have experienced large increases in air pollution levels and have large exposed populations.

We further evaluate the relative importance of changes in emissions of short-lived species, climate, and CH_4 concentrations in driving changes in $PM_{2.5}$, O_3 and associated premature mortalities.

We find that increases in short-lived air pollutant emissions from 1860 to 2000 lead to $7.5 \pm 0.19\,\mu g\,m^{-3}$ and $25 \pm 0.30\,ppbv$ increases in $PM_{2.5}$ and H-O_3 concentrations respectively, accounting for a majority (94 % and 83 %) of total increases in these two species over this period. Changes in emissions of short-lived pollutants account for over 95 % of all-cause mortalities associated with industrial $PM_{2.5}$ and over 85 % of respiratory mortalities associated with industrial O_3.

CH_4 concentration increase is the second most important driver of H-O_3 increases, causing an increase of $4.3 \pm 0.33\,ppbv$ and accounting for almost 15 % of the total increase of H-O_3 from 1860 to 2000. CH_4 contributes nearly 15 % of the total respiratory mortalities associated with industrial O_3. CH_4 has negligible effects on $PM_{2.5}$ and has an insignificant effect on total all-cause mortalities associated with $PM_{2.5}$.

Changing climate has a small role in driving O_3 change during the industrial period, causing an increase of 0.5 ± 0.28 ppbv (2 % of the total increase of H-O_3) from 1860 to 2000. Climate change is the second most important driver of changes in $PM_{2.5}$ during the industrial period, causing an increase of $0.4 \pm 0.17\,\mu g\,m^{-3}$ (5 % of its total increase) from 1860 to 2000. The effect of climate change on industrial air pollution mortalities is small but non-negligible for both $PM_{2.5}$ and O_3, accounting for less than 5 % and approximately 2 % of changes in mortality associated with these species during the industrial period, respectively.

The contribution together of climate change and CH_4 concentration increases to excess mortalities over various regions due to industrial air pollution ranges from 1 % to 13 % for all-cause mortality associated with industrial $PM_{2.5}$ and from 8 % to 33 % for respiratory mortality associated with O_3. In terms of respiratory mortalities associated with industrial O_3 exposure, increased CH_4 concentrations alone contribute more than 20 % over South America, Europe, Africa, Middle East and Rest of Asia. Recent projections indicate that over Europe and the United States local O_3 precursor emissions are likely to continue to decrease after 2000 (van der A et al., 2008; Richter et al., 2005). In the mean time, CH_4 is projected to increase in almost all SRES and RCP emission scenarios (except RCP2.6 and SRES B2). As a result, the relative contribution of increased CH_4 to O_3 mortality will likely continue to rise, increasing the relative health benefits of CH_4 mitigation.

Increases in CH_4 concentrations since preindustrial time are highly influential on the oxidizing capacity of the atmosphere, as CH_4 increases are the most important factor driving changes in both tropospheric OH and H_2O_2 abundance of all the factors discussed in this paper. Especially for OH, the primary atmospheric oxidant, historical increases in CH_4 drive its decreases, which will decrease its control of the buildup of reduced air pollutants such as CO and SO_2.

As the benefit of CH_4 reduction does not depend on its location, for cleaner regions, such as Europe, South America and Australia (where we find mortality burdens to be more sensitive to CH_4 concentration than other regions), identifying the least cost

CH$_4$ mitigation option internationally can be a highly cost-effective way to reduce their premature mortalities from O$_3$ exposure. Our study highlights the benefits of controlling CH$_4$ emissions as part of air quality policy.

Modeling estimates of industrial air pollution and associated excess mortalities strongly depend on emission changes applied during this time period, as reflected by differences between this study and Anenberg et al. (2010). They also depend on simulated physical, dynamical and chemical processes in the atmosphere. To evaluate the robustness of our results, similar studies using different chemistry-climate models could be conducted. Many of the simulations applied in this study were conducted under the Atmospheric Chemistry and Climate Model Intercomparison Project (ACCMIP). Multiple modeling groups have participated in this project, all of which use the same emission inventories and run simulations for preindustrial (1860) and present (2000) (http://www.giss.nasa.gov/projects/accmip/specifications.html). Further analysis of the ACCMIP simulations could reduce (refer to ACP special issue on ACCMIP) uncertainties in modeling estimates of industrial air pollution and associated mortalities.

Supplementary material related to this article is available online at: http://www.atmos-chem-phys-discuss.net/12/22713/2012/ acpd-12-22713-2012-supplement.pdf.

References

Andres, R. J., Fielding, D. J., Marland, G., Boden, T. A., Kumar, N., and Kearney, A. T.: Carbon dioxide emissions from fossil-fuel use, 1751–1950, Tellus B, 51, 759–765, doi:10.1034/j.1600-0889.1999.t01-3-00002.x, 1999.

Anenberg, S. C., Horowitz, L. W., Tong, D. Q., and West, J. J.: An estimate of the global burden of anthropogenic ozone and fine particulate matter on premature human mortality using atmospheric modeling, Environ. Health Persp., 118, 1189–1195, doi:10.1289/ehp.0901220, 2010.

Bell, M. L., McDermott, A., Zeger, S. L., Samet, J. M., and Dominici, F.: Ozone and short-term mortality in 95 US urban communities, 1987–2000, JAMA-J. Am. Med. Assoc., 292, 2372–2378, doi:10.1001/jama.292.19.2372, 2004.

Bell, M. L., Goldberg, R., Hogrefe, C., Kinney, P., Knowlton, K., Lynn, B., Rosenthal, J., Rosenzweig, C., and Patz, J.: Climate change, ambient ozone, and health in 50 US cities, Climatic Change, 82, 61–76, doi:10.1007/s10584-006-9166-7, 2007.

CIESIN, Center for International Earth Science Information Network: Columbia University; and Centro Internacional de Agricultura Tropical (CIAT), 2005, Gridded Population of the World, Version 3 (GPWv3). Palisades, NY: Socioeconomic Data and Applications Center (SEDAC), Columbia University, available at: http://sedac.ciesin.columbia.edu/gpw, last access: 30 August 2012.

Collins, W. J., Derwent, R. G., Garnier, B., Johnson, C. E., Sanderson, M. G., and Stevenson, D. S.: Effect of stratosphere-troposphere exchange on the future tropospheric ozone trend, J. Geophys. Res., 108, 8528, doi:10.1029/2002jd002617, 2003.

Dentener, F., Stevenson, D., Cofala, J., Mechler, R., Amann, M., Bergamaschi, P., Raes, F., and Derwent, R.: The impact of air pollutant and methane emission controls on tropospheric ozone and radiative forcing: CTM calculations for the period 1990–2030, Atmos. Chem. Phys., 5, 1731–1755, doi:10.5194/acp-5-1731-2005, 2005.

Donner, L. J., Wyman, B. L., Hemler, R. S., Horowitz, L. W., Ming, Y., Zhao, M., Golaz, J.-C., Ginoux, P., Lin, S.-J., Schwarzkopf, D. M., Austin, J., Alaka, G., Cooke, W. F., Delworth, T. L., Freidenreich, S. M., Gordon, C. T., Griffies, S. M., Held, I. M., Hurlin, W. J., Klein, S. A., Knutson, T. R., Langenhorst, A. R., Lee, H.-C., Lin, Y., Magi, B. I., Malyshev, S. L., Milly, P. C. D., Naik, V., Nath, M. J., Pincus, R., Ploshay, J. J., Ramaswamy, V., Seman, C. J., Shevliakova, E., Sirutis, J. J., Stern, W. F., Stouffer, R. J., Wilson, R. J., Winton, M., Wittenberg, A. T., and Zeng, F.: The dynamical core, physical parameterizations, and basic simulation characteristics of the atmospheric component AM3 of the GFDL Global Coupled Model CM3, J. Climate, 3484–3519, doi:10.1175/2011JCLI3955.1, 2011.

Döscher, A., Gäggeler, H. W., Schotterer, U., and Schwikowski, M.: A 130 yr deposition record of sulfate, nitrate and chloride from a high-alpine glacier, Water Air Soil Pollut., 85, 603–609, doi:10.1007/bf00476895, 1995.

Fang, Y., Fiore, A. M., Horowitz, L. W., Levy, H., II, Hu, Y., and Russell, A. G.: Sensitivity of the NO_y budget over the United States to anthropogenic and lightning NO_x in summer, J. Geophys. Res., 115, D18312, doi:10.1029/2010jd014079, 2010.

Title Page

Abstract | Introduction

Conclusions | References

Tables | Figures

◄ | ►

◄ | ►

Back | Close

Full Screen / Esc

Printer-friendly Version

Interactive Discussion

Fang, Y., Mauzerall, D. L., Liu, J., Fiore, A. M., and Horowitz, L. W.: Impacts of 21st century climate change on global air pollution-related premature mortality, Climatic Change, in review, 2012.

Fiore, A. M., Jacob, D. J., Field, B. D., Streets, D. G., Fernandes, S. D., and Jang, C.: Linking ozone pollution and climate change: the case for controlling methane, Geophys. Res. Lett., 29, 1919, doi:10.1029/2002gl015601, 2002.

Fiore, A. M., West, J. J., Horowitz, L. W., Naik, V., and Schwarzkopf, M. D.: Characterizing the tropospheric ozone response to methane emission controls and the benefits to climate and air quality, J. Geophys. Res., 113, D08307, doi:10.1029/2007jd009162, 2008.

Fischer, H., Wagenbach, D., and Kipfstuhl, J.: Sulfate and nitrate firn concentrations on the Greenland ice sheet, 2. temporal anthropogenic deposition changes, J. Geophys. Res., 103, 21935–21942, doi:10.1029/98jd01886, 1998.

Goldewijk, K. K.: Three centuries of global population growth: a spatial referenced population (density) database for 1700–2000, Popul. Environ., 26, 343–367, doi:10.1007/s11111-005-3346-7, 2005.

Grenfell, J. L., Shindell, D. T., Koch, D., and Rind, D.: Chemistry-climate interactions in the Goddard Institute for Space Studies general circulation model, 2. new insights into modeling the preindustrial atmosphere, J. Geophys. Res., 106, 33435–33451, doi:10.1029/2000jd000090, 2001.

Gros, V.: Background ozone and long distance transport of nitrogen oxides, global change magazine for schools, published by ACCENT, available at:http://www.atmosphere.mpg.de/enid/Nr2JuneO5_Research_5og.html (last access: August 2012), 2006.

HEI: Public Health and Air Pollution in Asia (PAPA): Coordinated Studies of Short-Term Exposure to Air Pollution and Daily Mortality in Four Cities, Health Effects Institute Boston, MA, USA, 2010.

Horowitz, L. W.: Past, present, and future concentrations of tropospheric ozone and aerosols: methodology, ozone evaluation, and sensitivity to aerosol wet removal, J. Geophys. Res., 111, D22211, doi:10.1029/2005jd006937, 2006.

IPCC: Climate Change 2001: The Scientific Basis. Contribution of Working Group I to the Third Assessment Report of the Intergovernmental Panel on Climate Change, edited by: Houghton, J. T., Ding, Y., Griggs, D. J., Noguer, M., van der Linden, P. J., Dai, X., Maskell, K., and Johnson, C. A., Cambridge University Press, Cambridge, United Kingdom, 1000 pp., 2001.

Jerrett, M., Burnett, R. T., Pope, A. C., Ito, K., Thurston, G., Krewski, D., Shi, Y., Calle, E., and Thun, M.: Long-Term Ozone Exposure and Mortality, New Engl. J. Med., 360, 1085–1095, doi:10.1056/NEJMoa0803894, 2009.

John, J. G., Fiore, A. M., Naik, V., Horowitz, L. W., and Dunne, J. P.: Climate versus emission drivers of methane lifetime from 1860–2100, Atmos. Chem. Phys. Discuss., 12, 18067–18105, doi:10.5194/acpd-12-18067-2012, 2012.

Krewski, D., Jerrett, M., Burnett, R. T., Ma, R., Hughes, E., Shi, Y., Turner, M. C., Pope, C. A., Thurston, G., Calle, E. E., Thun, M. J., Beckerman, B., DeLuca, P., Finkelstein, N., Ito, K., Moore, D. K., Newbold, K. B., Ramsay, T., Ross, Z., Shin, H., and Tempalski, B.: Extended follow-up and spatial analysis of the American Cancer Society study linking particulate air pollution and mortality, Health Effects Institute, Cambridge, MA, USA, 5–114, 2009.

Lamarque, J. F., Hess, P., Emmons, L., Buja, L., Washington, W., and Granier, C.: Tropospheric ozone evolution between 1890 and 1990, J. Geophys. Res., 110, D08304, doi:10.1029/2004jd005537, 2005.

Lamarque, J.-F., Bond, T. C., Eyring, V., Granier, C., Heil, A., Klimont, Z., Lee, D., Liousse, C., Mieville, A., Owen, B., Schultz, M. G., Shindell, D., Smith, S. J., Stehfest, E., Van Aardenne, J., Cooper, O. R., Kainuma, M., Mahowald, N., McConnell, J. R., Naik, V., Riahi, K., and van Vuuren, D. P.: Historical (1850–2000) gridded anthropogenic and biomass burning emissions of reactive gases and aerosols: methodology and application, Atmos. Chem. Phys., 10, 7017–7039, doi:10.5194/acp-10-7017-2010, 2010.

Lamarque, J.-F., Shindell, D. T., Josse, B., Young, P. J., Cionni, I., Eyring, V., Bergmann, D., Cameron-Smith, P., Collins, W. J., Doherty, R., Dalsoren, S., Faluvegi, G., Folberth, G., Ghan, S. J., Horowitz, L. W., Lee, Y. H., MacKenzie, I. A., Nagashima, T., Naik, V., Plummer, D., Righi, M., Rumbold, S., Schulz, M., Skeie, R. B., Stevenson, D. S., Strode, S., Sudo, K., Szopa, S., Voulgarakis, A., and Zeng, G.: The Atmospheric Chemistry and Climate Model Intercomparison Project (ACCMIP): overview and description of models, simulations and climate diagnostics, Geosci. Model Dev. Discuss., 5, 2445–2502, doi:10.5194/gmdd-5-2445-2012, 2012.

Lavanchy, V. M. H., Gäggeler, H. W., Schotterer, U., Schwikowski, M., and Baltensperger, U.: Historical record of carbonaceous particle concentrations from a European high-alpine glacier (Colle Gnifetti, Switzerland), J. Geophys. Res., 104, 21227–21236, doi:10.1029/1999jd900408, 1999.

Title Page

Abstract | Introduction

Conclusions | References

Tables | Figures

◄◄ | ►►

◄ | ►

Back | Close

Full Screen / Esc

Printer-friendly Version

Interactive Discussion

Levy, J. I., Chemerynski, S. M., and Sarnat, J. A.: Ozone Exposure and Mortality: "An Empiric Bayes Metaregression Analysis", Epidemiology, 16, 458–468, doi:10.1097/01.ede.0000165820.08301.b3, 2005.

Liao, H., Chen, W.-T., and Seinfeld, J. H.: Role of climate change in global predictions of future tropospheric ozone and aerosols, J. Geophys. Res., 111, D12304, doi:10.1029/2005jd006852, 2006.

Lin, M., Fiore, A. M., Horowitz, L. W., Cooper, O. R., Naik, V., Holloway, J., Johnson, B. J., Middlebrook, A. M., Oltmans, S. J., Pollack, I. B., Ryerson, T. B., Warner, J. X., Wiedinmyer, C., Wilson, J., and Wyman, B.: Transport of Asian ozone pollution into surface air over the Western United States in spring, J. Geophys. Res., 117, D00V07, doi:10.1029/2011jd016961, 2012.

Liu, J., Mauzerall, D. L., Horowitz, L. W., Ginoux, P., and Fiore, A. M.: Evaluating intercontinental transport of fine aerosols: (1) methodology, global aerosol distribution and optical depth, Atmos. Environ., 43, 4327–4338, doi:10.1016/j.atmosenv.2009.03.054, 2009.

Marenco, A., Gouget, H., Nédélec, P., Pagés, J.-P., and Karcher, F.: Evidence of a long-term increase in tropospheric ozone from Pic du Midi data series: consequences: positive radiative forcing, J. Geophys. Res., 99, 16617–16632, doi:10.1029/94jd00021, 1994.

Marlon, J. R., Bartlein, P. J., Carcaillet, C., Gavin, D. G., Harrison, S. P., Higuera, P. E., Joos, F., Power, M. J., and Prentice, I. C.: Climate and human influences on global biomass burning over the past two millennia, Nat. Geosci., 1, 697–702, available at: http://www.nature.com/ngeo/journal/v1/n10/suppinfo/ngeo313_S1.html, 2008.

McConnell, J. R., Edwards, R., Kok, G. L., Flanner, M. G., Zender, C. S., Saltzman, E. S., Banta, J. R., Pasteris, D. R., Carter, M. M., and Kahl, J. D. W.: 20th-century industrial black carbon emissions altered arctic climate forcing, Science, 317, 1381–1384, doi:10.1126/science.1144856, 2007.

Meinshausen, M., Smith, S., Calvin, K., Daniel, J., Kainuma, M., Lamarque, J. F., Matsumoto, K., Montzka, S., Raper, S., Riahi, K., Thomson, A., Velders, G., and van Vuuren, D. P.: The RCP greenhouse gas concentrations and their extensions from 1765 to 2300, Climatic Change, 109, 213–241, doi:10.1007/s10584-011-0156-z, 2011.

Mickley, L. J., Jacob, D. J., and Rind, D.: Uncertainty in preindustrial abundance of tropospheric ozone: implications for radiative forcing calculations, J. Geophys. Res., 106, 3389–3399, doi:10.1029/2000jd900594, 2001.

Title Page

Abstract | Introduction

Conclusions | References

Tables | Figures

◄ | ►►

◄ | ►

Back | Close

Full Screen / Esc

Printer-friendly Version

Interactive Discussion

Mieville, A., Granier, C., Liousse, C., Guillaume, B., Mouillot, F., Lamarque, J. F., Grégoire, J. M., and Pétron, G.: Emissions of gases and particles from biomass burning during the 20th century using satellite data and an historical reconstruction, Atmos. Environ., 44, 1469–1477, doi:10.1016/j.atmosenv.2010.01.011, 2010.

5   Murazaki, K. and Hess, P.: How does climate change contribute to surface ozone change over the United States?, J. Geophys. Res., 111, D05301, doi:10.1029/2005jd005873, 2006.

Naik, V., Horowitz, L. W., Fiore, A. M., Mao, J., Aghedo, A., and Levy, H. I.: Preindustrial to present day impact of short-lived pollutant emissions on atmospheric composition and climate, J. Geophys. Res.-Atmos., submitted, 2012.

10   Nakicenovic, N., Alcamo, J., Davis, G., de Vries, B., Fenhann, J., Gaffin, S., Kenneth Gregory, Grübler, A., Jung, T. Y., Kram, T., Rovere, E. L. L., Michaelis, L., Mori, S., Morita, T., Pepper, W., Pitcher, H., Price, L., Riahi, K., Roehrl, A., Rogner, H.-H., Sankovski, A., Schlesinger, M., Shukla, P., Smith, S., Swart, R., van Rooijen, S., Victor, N., and Zhou, D.: Special Report on Emissions Scenarios: A Special Report of Working Group III of the Intergovernmental Panel

15   on Climate Change, Cambridge University Press, Cambridge, UK, 599 pp., 2000.

Pope, C. A. and Dockery, D. W.: Health effects of fine particulate air pollution: lines that connect, J. Air Waste Manage. Assoc., 56, 709–742, 2006.

Pope, C. A., Burnett, R. T., Thun, M. J., Calle, E. E., Krewski, D., Ito, K., and Thurston, G. D.: Lung Cancer, Cardiopulmonary Mortality, and Long-term Exposure to Fine Particulate Air

20   Pollution, J. Amer. Med. Assoc., 287, 1132–1141, doi:10.1001/jama.287.9.1132, 2002.

Ramaswamy, V., Boucher, O., Haigh, J., Hauglustaine, D., Haywood, J., Myhre, G., Nakajima, T., Shi, G. Y., Solomon, S., Betts, R., Charlson, R., Chuang, C., Daniel, J. S., Genio, A. D., Dorland, R. v., Feichter, J., Fuglestvedt, J., Forster, P. M. d. F., Ghan, S. J., Jones, A., Kiehl, J. T., Koch, D., Land, C., Lean, J., Lohmann, U., Minschwaner, K., Penner, J. E., Roberts, D.

25   L., Rodhe, H., Roelofs, G. J., Rotstayn, L. D., Schneider, T. L., Schumann, U., Schwartz, S. E., Schwarzkopf, M. D., Shine, K. P., Smith, S., Stevenson, D. S., Stordal, F., Tegen, I., and Zhang, Y.: Radiative forcing of climate change, in: Climate Change 2001: The Scientific Basis. Contribution of Working Group I to the Third Assessment Report of the Intergovernmental Panel on Climate Change, edited by: Houghton, J. T., Ding, Y., Griggs, D. J., Noguer, M.,

30   Linden, P. J. v. d., Dai, X., Maskell, K., and Johnson, C. A., Cambridge University Press, Cambridge, UK, 881 pp., 2001.

Title Page

Abstract | Introduction

Conclusions | References

Tables | Figures

◄ | ►►

◄ | ►

Back | Close

Full Screen / Esc

Printer-friendly Version

Interactive Discussion

Richter, A., Burrows, J. P., Nusz, H., Granier, C., and Niemeier, U.: Increase in tropospheric nitrogen dioxide over China observed from space, Nature, 437, 129–132, doi:10.1038/nature04092, 2005.

Schultz, M. G., Heil, A., Hoelzemann, J. J., Spessa, A., Thonicke, K., Goldammer, J. G., Held, A. C., Pereira, J. M. C., and van het Bolscher, M.: Global wildland fire emissions from 1960 to 2000, Global Biogeochem. Cy., 22, GB2002, doi:10.1029/2007gb003031, 2008.

Sigg, A., and Neftel, A.: Evidence for a 50 % increase in H_2O_2 over the past 200 yr from a Greenland ice core, Nature, 351, 557–559, 1991.

Staffelbach, T., Neftel, A., Stauffer, B., and Jacob, D.: A record of the atmospheric methane sink from formaldehyde in polar ice cores, Nature, 349, 603–605, 1991.

Tagaris, E., Liao, K.-J., DeLucia, A. J., Deck, L., Amar, P., and Russell, A. G.: Potential Impact of Climate Change on Air Pollution-Related Human Health Effects, Environ. Sci. Technol., 43, 4979–4988, doi:10.1021/es803650w, 2009.

Tsigaridis, K., Krol, M., Dentener, F. J., Balkanski, Y., Lathière, J., Metzger, S., Hauglustaine, D. A., and Kanakidou, M.: Change in global aerosol composition since preindustrial times, Atmos. Chem. Phys., 6, 5143–5162, doi:10.5194/acp-6-5143-2006, 2006.

van der A, R. J., Eskes, H. J., Boersma, K. F., van Noije, T. P. C., Van Roozendael, M., De Smedt, I., Peters, D. H. M. U., and Meijer, E. W.: Trends, seasonal variability and dominant NO_x source derived from a ten year record of NO_2 measured from space, J. Geophys. Res., 113, D04302 doi:10.1029/2007jd009021, 2008.

van der Werf, G. R., Randerson, J. T., Giglio, L., Collatz, G. J., Kasibhatla, P. S., and Arellano Jr., A. F.: Interannual variability in global biomass burning emissions from 1997 to 2004, Atmos. Chem. Phys., 6, 3423–3441, doi:10.5194/acp-6-3423-2006, 2006.

Wang, Y. and Jacob, D. J.: Anthropogenic forcing on tropospheric ozone and OH since preindustrial times, J. Geophys. Res., 103, 31123–31135, doi:10.1029/1998jd100004, 1998.

West, J. J., Fiore, A. M., Horowitz, L. W., and Mauzerall, D. L.: Global health benefits of mitigating ozone pollution with methane emission controls, P. Natl. Acad. Sci. USA, 103, 3988–3993, doi:10.1073/pnas.0600201103, 2006.

WHO: Global Burden of Disease (GBD) 2000: version 3 estimates, available at: http://www.who.int/healthinfo/global_burden_disease/estimates_regional_2000_v3/en/index.html (last access: August 2012), 2003.

Air pollution and associated human mortality

Y. Fang et al.

Title Page

Abstract	Introduction
Conclusions	References
Tables	Figures

◀ ▶

◀ ▶

Back | Close

Full Screen / Esc

Printer-friendly Version

Interactive Discussion

Zeng, G. and Pyle, J. A.: Changes in tropospheric ozone between 2000 and 2100 modeled in a chemistry-climate model, Geophys. Res. Lett., 30, 1392, doi:10.1029/2002gl016708, 2003.

Air pollution and associated human mortality

Y. Fang et al.

Title Page

Abstract | Introduction

Conclusions | References

Tables | Figures

◄ | ►►

◄ | ►

Back | Close

Full Screen / Esc

Printer-friendly Version

Interactive Discussion

Table 1. Model simulation configurations. All simulations are run for 11 yr with the first year used for spin-up (SST: sea surface temperature; SIC: sea ice; WMGG: well mixed greenhouse gases; ODS: ozone depleting substances).

	Simulations	SST and SIC	WMGG	ODS[a]	CH_4 (tropospheric chemistry)	Anthropogenic and biomass burning emissions
1	2000[b]	2000	2000	2000	2000	2000
2	1860[b]	1860	1860	1860	1860	1860
3	2000CL1860EM	2000	2000	2000	2000	1860
4	1860CL2000EM[b]	1860	1860	1860	2000	2000
5	1860ALL2000EM	1860	1860	1860	1860	2000

[a] The 1860 level of Ozone Depleting Substances is set to pre-1950 levels.
[b] Simulations run for the Atmospheric Chemistry and Climate Model Inter-comparison Project (ACCMIP).

Table 2. Concentration-response relationships used to estimate changes in premature mortality associated with changes in air pollutant concentrations.

Pollutant	Study and reference	Cause of Death	Exposure Indicator in epidemiological study and applied in our work (in parentheses)	Age Group	β value (%) with its 95 % CI (in parentheses)
$PM_{2.5}$	ACS[a] Long-term cohort (Krewski et al., 2009)	All-cause	Long-term average (annual mean)	≥ 30	6 (4–8)[b]
O_3	ACS Long-term cohort (Jerrett et al., 2009)	Respiratory disease	Health-relevant O_3 (defined as maximum 6-month mean of 1-h daily maximum O_3 in a year)	≥ 30	4 (1.3–6.7)[c]

[a] American Cancer Society.
[b] Per $10\,\mu g\,m^{-3}$ increase in $PM_{2.5}$.
[c] Per 10 ppbv increase in O_3.

Title Page

Abstract | Introduction

Conclusions | References

Tables | Figures

|◄ | ►|

◄ | ►

Back | Close

Full Screen / Esc

Printer-friendly Version

Interactive Discussion

Table 3. Year 2000 global population-weighted annual mean surface $PM_{2.5}$ and $H\text{-}O_3$ (health-relevant O_3, defined in Sect. 2), tropospheric mean mass-weighted OH and H_2O_2 concentrations, and their changes from 1860 to 2000 driven by all changes (TOTAL), changes in emissions of short-lived reactive pollutants (EMIS), changes in climate (CLIM), and changes in tropopsheric CH_4 concentration(TCH_4). Results are reported for 10-yr model simulations as annual average ± standard deviation.

Atmospheric species	2000	TOTAL	EMIS	CLIM	TCH_4
$PM_{2.5}$ ($\mu g\,m^{-3}$)	13 ± 0.15	8 ± 0.16	7.5 ± 0.19	0.4 ± 0.17	0.04 ± 0.24
$H\text{-}O_3$(ppbv)	61 ± 0.20	30 ± 0.16	25 ± 0.30	0.5 ± 0.28	4.3 ± 0.33
OH (10^6 molecules cm^{-3})	1.19 ± 0.01	−0.11 ± 0.01	0.13 ± 0.01	−0.02 ± 0.01	−0.24 ± 0.01
H_2O_2 (10^{10} molecules cm^{-3})	1.95 ± 0.01	0.84 ± 0.01	0.41 ± 0.02	0.15 ± 0.03	0.35 ± 0.02

Table 4. Premature mortalities in 2000 associated with industrial air pollution. Values are calculated as in Eq. (1), using ACS health impact functions, concentration difference in annual $PM_{2.5}$ and $H\text{-}O_3$ between "1860" and 2000" simulations, WHO baseline mortality rate and population in the year 2000. The 95 % confidence intervals are shown in brackets.

Change in Premature mortalities (1000s deaths)	$PM_{2.5}$ mortality (Chronic, all-cause)	O_3 mortality (Chronic, respiratory)
World	1518 (1033, 1983)	375 (129, 592)
North America	38 (25, 49)	26 (9, 41)
South America	17 (12, 23)	5 (2, 8)
Europe	98 (66, 129)	31 (11, 49)
Africa	114 (77, 150)	19 (6, 30)
South Asia	437 (298, 570)	70 (24, 111)
Southeast Asia	118 (80, 154)	27 (9, 43)
East Asia	620 (424, 808)	183 (64, 287)
Middle East	40 (27, 52)	7.5 (2.6, 12.0)
Rest of Asia	20 (14, 27)	5.5 (2.6, 8.8)
Australia	0.7 (0.5, 0.9)	0.3 (0.1, 0.4)
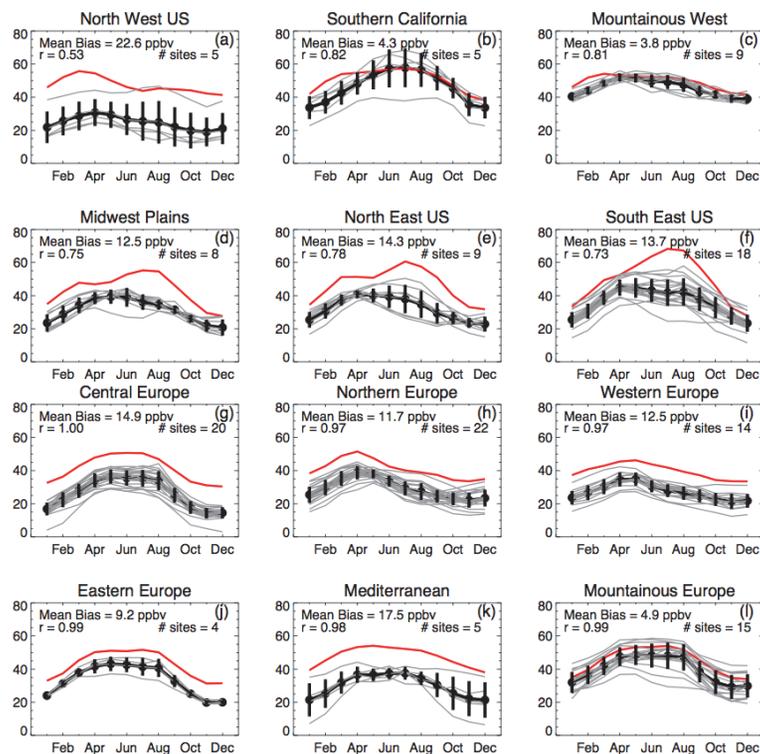
Fig. 1. Comparison of simulated monthly mean surface O_3 in GFDL AM3 "2000" simulation (red line) with measurements from various regions in the United States (**a–f**, results from CASTNet, http://www.epa.gov/castnet/) and Europe (**g–l**, results from EMEP, http://www.nilu.no/projects/ccc/emepdata.html). Observed values (black dots) represent the average of climatological monthly mean surface O_3 concentrations for each site (grey lines) within each region (Table S1 in Naik et al., 2012). Vertical black lines denote standard deviation across the sites.
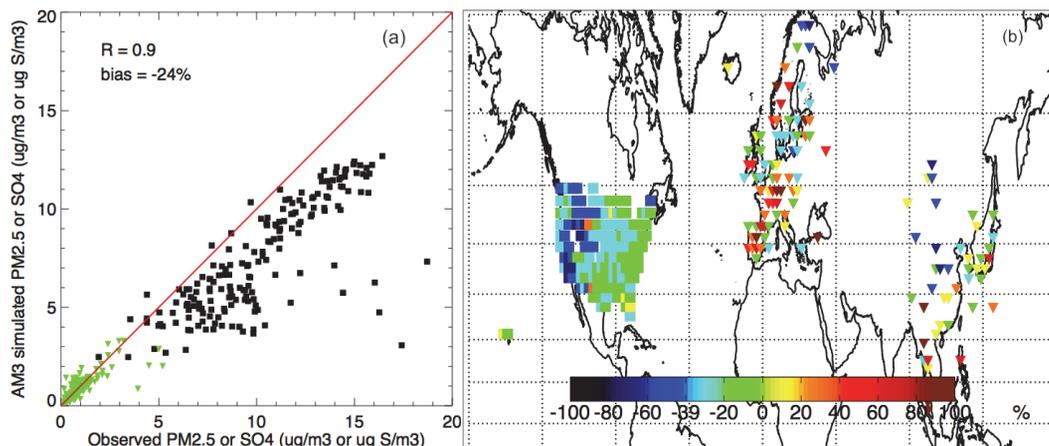
Fig. 2. (a) Scatter plot of AM3 "2000" simulated and observed annual mean concentrations of $PM_{2.5}$ (black squares) or sulfate (green triangles). 1 : 1 line is shown in red. **(b)** Map of the relative difference (i.e., (model-obs)/obs) in $PM_{2.5}$ (squares) or sulfate (triangles). $PM_{2.5}$ observations over the United States are from the U.S. Air Quality System (AQS) Database (1997–2003 average, http://www.epa.gov/ttn/airs/airsaqs/); sulfate observations over Europe are from the European Monitoring and Evaluation Programme (EMEP, 1995–2004, http://www.emep.int/). Sulfate observations over East Asia are from the Acid Deposition Monitoring Network in East Asia (EANET, http://www.eanet.cc/product/index.html), collected from Liu et al. (2009) and Zhang et al. (2011).
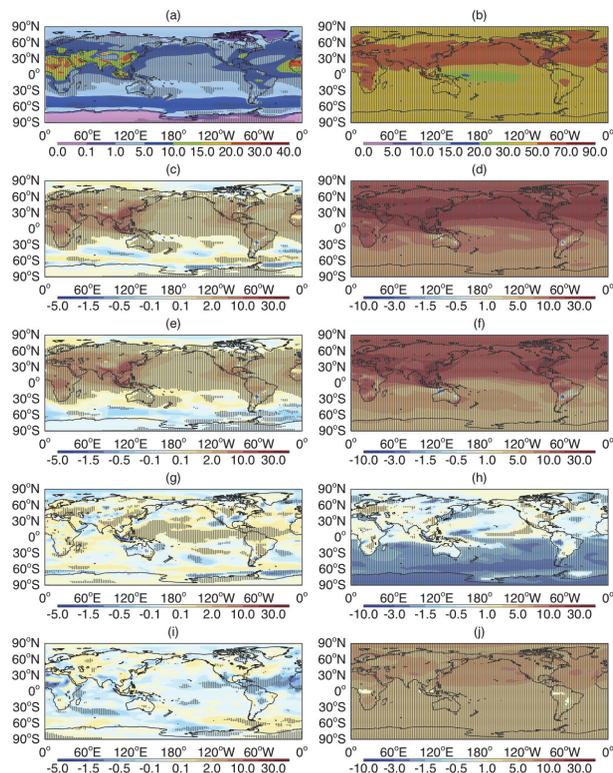
Fig. 3. Annual PM$_{2.5}$ (left, unit: μg m^{-3}) and H-O$_3$ (right, unit: ppbv) surface concentration in 2000 (row 1, **a** and **b**), their total changes from preindustrial to present day ("2000" minus "1860" simulations) (row 2, **c** and **d**), and changes over that time interval due to anthropogenic air pollutant emissions only ("2000" minus "2000CL1860EM" simulations) (row 3, **e** and **f**), due to climate change only ("2000" minus "1860CL2000EM" simulations) (row 4, **g** and **h**), and due to the impact of CH$_4$ increases on tropospheric chemistry only ("1860CL2000EM" minus "1860ALL2000EM" simulations) (row 5, **i** and **j**). Dotted areas indicate changes significant at the 95 % confidence level as assessed by student t test.

Title Page

Abstract | Introduction

Conclusions | References

Tables | Figures

◄◄ | ►►

◄ | ►

Back | Close

Full Screen / Esc
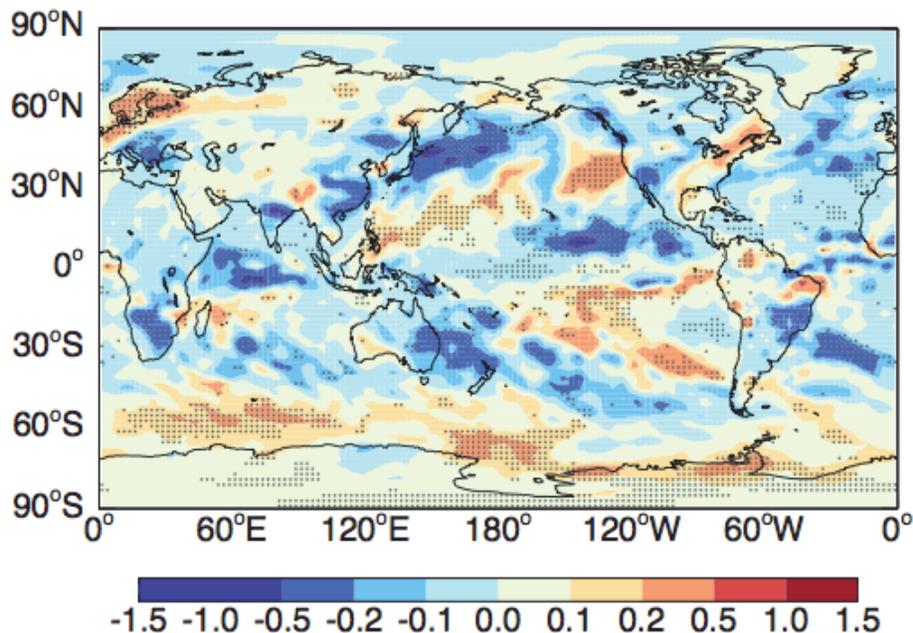
Printer-friendly Version

Interactive Discussion

Fig. 4. Changes in annual mean stratiform (large-scale) precipitation (unit: mm day^{-1}) driven by climate change (derived as "2000" – "1860CL2000emis" simulations). Dotted areas indicate changes significant at the 95 % confidence level as assessed by student t-test.
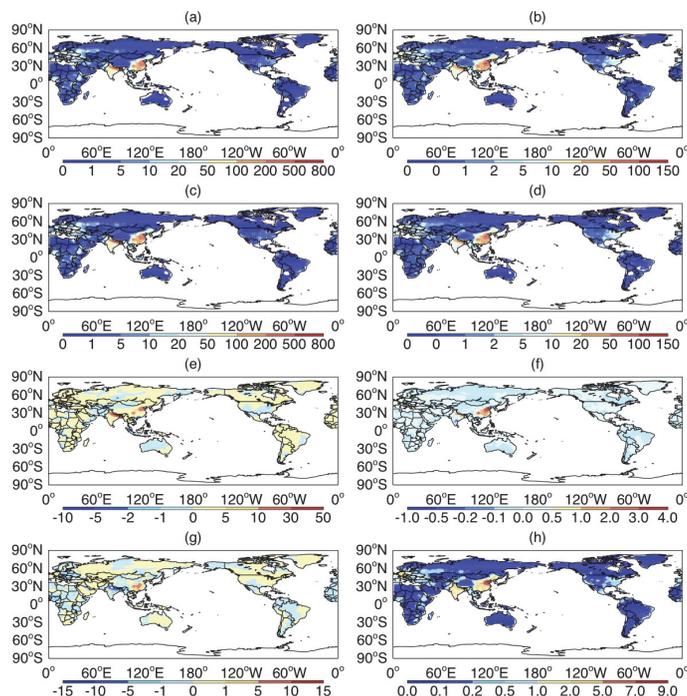
Fig. 5. Annual premature deaths (unit: deaths/1000 km^2 attributed to total changes in PM$_{2.5}$ (left) and O$_3$ (right) from preindustrial to present ("2000" minus "1860" simulations) (row 1, **a** and **b**), and changes in PM$_{2.5}$ and O$_3$ over that time interval due to increases in short-lived anthropogenic air pollutant emissions only ("2000" minus "2000CL1860EM" simulations) (row 2, **c** and **d**), due to climate change only ("2000" minus "1860CL2000EM" simulations) (row 3, **e** and **f**), and due to the impact of CH$_4$ increases on tropospheric chemistry only ("1860CL2000EM" minus "1860ALL2000EM" simulations) (row 4, **g** and **h**).

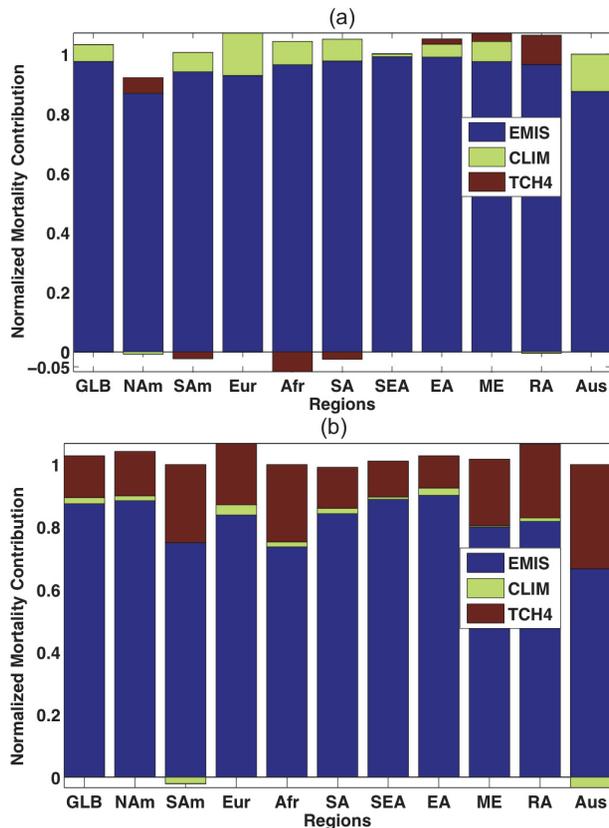**Fig. 6.** Normalized Mortality Contribution over each region associated with surface **(a)** $PM_{2.5}$ and **(b)** O_3. Blue, green and dark red represent the impact of changes in emissions of short-lived species, climate change and the impact of CH_4 change on tropospheric chemistry, respectively. Labels on the x-axis represent the following global regions: Globe, North America, South America, Europe, Africa, South Asia, Southeast Asia, East Asia, Middle East, Rest of Asia, and Australia, as in Fang et al. (2012).